Behavioural Brain Research 409 (2021) 113324

Contents lists available at ScienceDirect

Behavioural Brain Research

journal homepage: www.elsevier.com/locate/bbr

Research report

Hyperhomocysteinemia increases susceptibility to cortical spreading depression associated with photophobia, mechanical allodynia, and anxiety in rats

Elena Gerasimova [a], Gulshat Burkhanova [b], Kseniya Chernova [b], Andrey Zakharov [c,b], Daniel Enikeev [a], Nail Khaertdinov [a], Rashid Giniatullin [b,d], Guzel Sitdikova [a,*]

[a] Department of Human and Animal Physiology, Institute of Fundamental Medicine and Biology, Kazan Federal University, Kazan, Russia
[b] Laboratory of Neurobiology, Institute of Fundamental Medicine and Biology, Kazan Federal University, Kazan, Russia
[c] Department of Physiology, Kazan State Medical University, Kazan, Russia
[d] A.I.Virtanen Institute, University of Eastern, Finland, Kuopio, Finland

ARTICLE INFO

Keywords:
Migraine
Hyperhomocysteinemia
Cortical spreading depression
Cortical excitability
Allodynia
Anxiety

ABSTRACT

Epidemiological data suggest that elevated homocysteine is associated with migraine with aura. However, how homocysteine contributes to migraine is still unclear. Here, we tested whether hyperhomocysteinemia (hHCY) promotes cortical spreading depression (CSD), a phenomenon underlying migraine with aura, and whether hHCY contributes to pain behavior. hHCY was induced by dietary methionine in female rats while the testing was performed on their 6–8week-old offspring. CSD and multiple unit activity (MUA) induced by KCl were recorded from the primary somatosensory cortex, S1, using multichannel electrodes. In hHCY rats, compared to control, we found: i) higher probability of CSD occurrence; ii) induction of CSD by lower concentrations of KCl; iii) faster horizontal propagation of CSD; iv) smaller CSD with longer duration; v) higher frequency of MUA at CSD onset along with slower reappearance. Rats with hHCY demonstrated high level of locomotor activity and grooming while spent less time in the central area of the open field, indicating anxiety. These animals showed light sensitivity and facial mechanical allodinia. Thus, hHCY acquired at birth promotes multiple features of migraine such as higher cortical excitability, mechanical allodynia, photophobia, and anxiety. Our results provide the first experimental explanation for the higher occurrence of migraine with aura in patients with hHCY.

1. Introduction

Homocysteine (HCY) is an endogenous redox active amino acid that is produced in the metabolic cycle of methionine by a transmethylation reaction. HCY then undergoes transsulfuration by cystathionine β-synthase (CBS) and this reaction requires pyridoxine (vitamin B6) as an enzymatic cofactor. Homocysteine can be remethylated into methionine in a reaction catalyzed by methionine synthase and methylenetetrahyrdofolate reductase (MTHFR) with vitamin B12 as a cofactor; folate is also required for this reaction [1]. Chronic hyperhomocysteinemia (hHCY) is an elevation of the HCY level in plasma with a number of causes, including genetic mutations in the MTHFR or CBS enzymes, nutritional deficiencies of vitamins (folate, B12 and B6), increased consumption of methionine, and aging [2]. hHCY is a well-known independent risk factor for cardio-vascular diseases and neurodegenerative disorders, and is associated with adverse pregnancy outcomes and common pregnancy complications such as preeclampsia [3].

The association between migraine and HCY levels was evaluated in population studies which demonstrated ambiguous results [4,5]. In some studies, higher HCY plasma levels in patients with migraine with aura were reported [6,7]. In another study, the HCY plasma level was not higher in a sample of migraineurs in a mixed group of patients with and without aura, although analysis by gender showed that HCY levels were higher in men [8]. The controversial data may be explained by the

Abbreviations: hHCY, hyperhomocysteinemia; CSD, cortical spreading depression; MUA, multiple unit activity; MTHFR, methylenetetrahyrdofolate reductase; LFP, local field potential.

* Corresponding author at: Guzel Sitdikova Department of Human and Animal Physiology, Institute of Fundamental Medicine and Biology, Kazan Federal University, Kazan, 420008, Kremlevskaya, 18, Russia.
E-mail address: sitdikovaguzel@gmail.com (G. Sitdikova).

https://doi.org/10.1016/j.bbr.2021.113324
Received 18 November 2020; Received in revised form 23 April 2021; Accepted 23 April 2021
Available online 26 April 2021

type of migraine (with or without aura), gender differences of HCY level, and accumulation of HCY derivatives in tissues during hHCY. Notably, total HCY concentration in the cerebrospinal fluid was significantly increased for both the migraine patients without and with aura [9]. Moreover, it was suggested that hHCY may represent a link between migraine with aura and risk of ischemic stroke [7,10]. Recent meta-analysis suggested a possible link between elevated serum HCY level and migraine, especially migraine with aura [11].

Cortical spreading depression (CSD) is a slowly propagating wave of transient neuronal and glial depolarization evoked by elevation of extracellular K^+ concentration, for example, by transient ischemia [12]. There is growing evidence that CSD underlies migraine with aura and possibly acts as a trigger for headache as well [13,14]. In neurological disorders such as migraine, cerebral ischemia, and traumatic brain injury, CSD plays a key role as a pathophysiological mechanism in brain damage [12]. An association between anxiety/depression and migraine, especially migraine with aura has been suggested in clinical studies [15–17]. Cutaneous allodynia is often reported in persons with frequent headache, indicating central sensitization which lowers the threshold for migraine triggers [18,19]. Recently we revealed mechanical allodynia in rats with prenatal hHCY which was reversed by inhibition of T-type Ca^{2+}-channels [20]. Notably, rats with chronic migraine showed depression and anxiety symptoms associated with susceptibility to CSD [21–23].

In this work, we evaluated the properties of CSD and multiple unit activity (MUA) in the somatosensory cortex of rats with prenatal hHCY. We also assessed if CSD susceptibility is accompanied by changes in light sensitivity, anxiety level, and facial allodynia which are the typical symptoms of migraine.

2. Materials and methods

2.1. The model of prenatal hHCY

Experiments were performed on Wistar rats in accordance with EU Directive 2010/63/EU for animal experiments and the Local Ethical Committee of KFU (protocol N№ 8 from 5.05.2015). Animals were housed in polyethylene cages at room temperature (22 °C) with a 12 -h light/dark cycle (lights on at 6 a.m.) and free access to water and food. In total 85 male rats at the age of 6–8 weeks were used in our experiments. Rats of the control group were born from females (n = 6) that were fed ad libitum with a control diet. Rats with prenatal hHCY (hHCY group) were born from females (n = 9) which received daily methionine (7.7 g/kg body weight) with food starting three weeks prior to, and during pregnancy [24–26]. Plasma HCY levels were measured in all dams and in randomly selected animals from their litters. Total HCY level in plasma was determined using a glass carbon electrode modified with multi-walled carbon nanotubes (MWNT/GCE) under conditions of square-wave voltammeter (Eco Chemie B.V., The Netherlands) [27]. HCY concentration was elevated in dams fed with the methionine diet (21 ± 3 μM; n = 9) compared to controls (7 ± 1 μM; n = 6). The HCY level in litters from the control group was 6.4 ± 0.9 μM (n = 9) whereas in the hHCY group it was 18.1 ± 0.8 μM (n = 9). The weight of rats from the control group was 139 ± 5 g (n = 39) and the weight of hHCY group – 95 ± 4 g (n = 38, $p < 0.05$). Electrophysiological and behavioral experiments were conducted on different groups of animals.

2.2. Surgery

Preparation of the animals for head-restrained recordings were as described previously [28–30]. Surgery was performed under isoflurane (Baxter, USA) anesthesia (5% induction and 2–3 % for maintenance) using anesthesia machine (E–Z anesthesia, World Precision Instruments, USA). Urethane (1.5 g/kg i.p.) was injected by the end of surgery and additional doses were delivered as necessary to maintain a surgical plane of anesthesia. The body temperature was maintained at 37 °C ± 0.5 °C using a self-regulating heating pad (TCAT-2LV controllers, Physitemp Instruments INC, USA). The head was fixed to the frame of a stereotaxic apparatus by the attached bars and two 2 mm diameter holes were drilled on the left side: one above the somatosensory cortex for electrophysiological recordings (3.5 mm posterior and 4 mm lateral to bregma) and the second for the chemical induction of CSD (8 mm posterior and 4 mm lateral to the bregma) (Fig.1 A). To determine horizontal CSD velocity two recording electrodes were inserted into the cortex (3.5 mm and 8 mm posterior and 4 mm lateral to bregma) and KCl was applied in a hole in the frontal bone (5 mm anterior and 4 mm

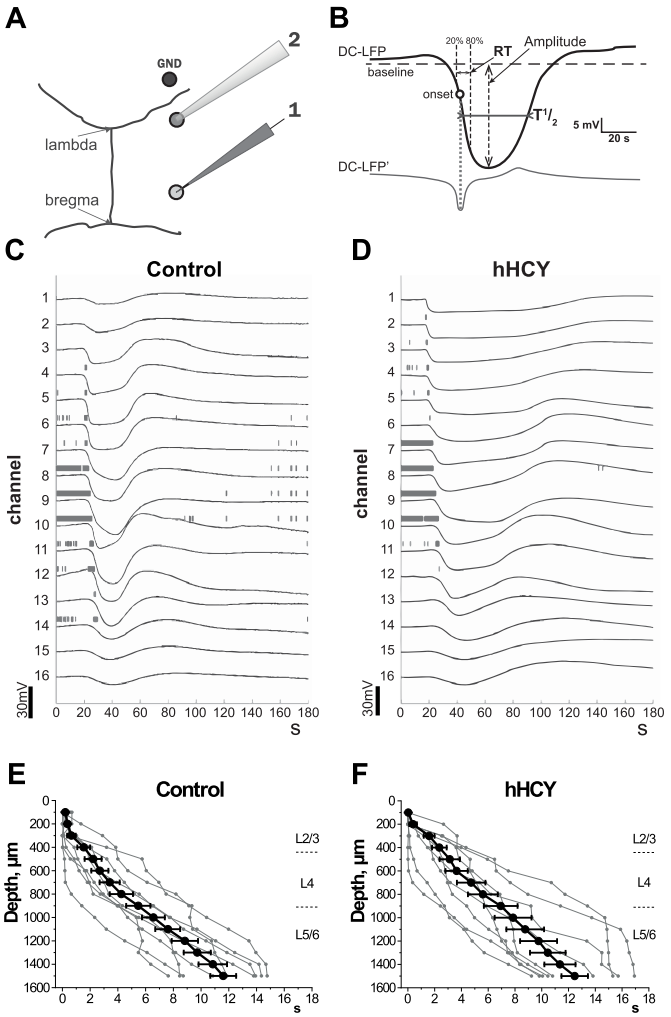

Fig. 1. *in vivo* **recording of cortical spreading depression (CSD) induced by KCl application**. **A.** Experimental design. CSD was recorded using a 16-site linear silicon probe (1) inserted in the somatosensory cortex (S1, 3.5 mm posterior and 4 mm lateral to bregma). KCl (2) was applied into an additional hole 4.5 mm posterior to the recording site. The ground electrode (GND) was placed in the visual cortex. **B.** Schematic trace of CSD (DC-LFP, top black trace) and its first derivative (DC-LFP', bottom grey trace) with the following analyzed parameters: onset (the negative peak time of the first LFP derivative), amplitude (the maximal negative LFP peak from the baseline), half-duration ($T_{1/2}$, duration at half amplitude), rise time (RT, time between 20 % and 80 % of CSD amplitude). The horizontal dashed line shows the baseline. **C,D.** An example of KCl-induced CSD recorded by 16-site linear silicon probe (100 μm distance between recording sites) in all layers of the cortical column in rats of the control (C) and hHCY (D) groups. The MUA marked by vertical grey lines were detected as negative events exceeding eight standard deviations in amplitude. **E,F.** Individual (grey circles) and average (black circles) CSD onsets at different cortical depths in animals from the control (E, n = 9) and hHCY (F, n = 9) groups. Time = 0 corresponds to the earliest CSD onset detected through all channels.

lateral to bregma) (Fig. 3 A inset). A chlorided silver wire, placed in the cerebellum or visual cortex served as a ground electrode. Before the recordings, the cortex was allowed to recover for 40 min. Respiratory rate under anesthesia was measured using piezoelectric transducer and it was not significantly different in control and hHCY animals (114 ± 12 in control, n = 3 versus 120 ± 12 in hHCY, n = 4, $p > 0.05$).

2.3. Electrophysiological recordings of CSD and data analysis

Slow direct current (DC) potential changes and spontaneous electrical activity were recorded using a 16-site linear silicon probe (A1 × 16−5mm-100−413 with 413 mm^2 iridium electrode site surface and 100 μm electrode separation distance, Neuronexus Technologies, Ann Arbor, MI, USA) in DC mode (Neuralynx, Bozeman, MO) which was inserted into the cortex to a depth of 1700 ± 100 μm [29]. This approach allowed us to analyze the electrical activity in all layers of somatosensory cortex (S1) and to determine the site of CSD initiation and its propagation along the cortical layers (Fig. 1. C,D). The layer division of the recording sites was defined by the cortical depth: 100−500 μm – supragranular layer (L2/3), 500−800 μm granular layer (L4), 900−1600 μm - infragranular layer (L5/6) [29,31].

CSD was induced by application of a 10 μL drop of KCl solution at increasing concentrations (10, 50, 100, 300, 600, and 1000 mM) into the posterior hole (Fig.1 A). Initially, 10 mM KCl was applied, and we observed whether CSD was induced for 10 min. If CSD was not induced after 10 min of observation, we removed KCl and washed the hole with artificial cerebrospinal fluid for 20 min before the next concentration was applied. If CSD appeared we recorded brain activity another 20 min after the last CSD occurrence and then washed the hole for 20 min before we progressed to a higher KCl concentration [32]. We measured the threshold of KCl concentration that induced CSD, the number and the duration of CSD occurrence in response to each concentration of KCl.

CSD recorded using a 16-site linear silicon probe consisted of waves of depolarization which spread along the layers of the cortical column (Fig. 1 C,D). From the original signal recorded in the DC mode (bandwidth 0−9000 Hz) the DC component was subtracted using the locdetrend procedure from chronux toolbox (MATLAB, the length of the sliding window was 120 s). CSD detection was performed visually by typical deflections of local field potential (LFP). Baseline level was calculated for each recording site as the mean LFP value in the time window between 20 and 10 s preceding CSD. For each recording site, the local negative peak time of the first LFP derivative within the 20 s time window preceding the negative CSD peak was considered as CSD onset (Fig.1 B). The amplitude-temporal parameters of the first CSD in each experiment were analyzed. CSD amplitude as the maximal negative LFP peak from the baseline, and CSD half-duration ($T_{1/2}$) as CSD duration at its half amplitude, were calculated (Fig. 1 B). We also assessed CSD rise time as the time between 20 % and 80 % of CSD amplitude (Fig. 1 B), and CSD depolarization rate calculated as the first LFP derivative value at the CSD onset time, normalized to CSD amplitude (μV/ms) [29]. The mean value of data obtained from the recording sites of each layer was used for statistical analysis.

To evaluate the horizontal velocity of CSD, a drop of 300 mM KCl was applied through the hole in the frontal bone to the cortex and CSDs were recorded for 60 min by two electrodes inserted into the cortex (Fig. 3 A inset). The rate of CSD propagation was calculated from the time required for the first CSD generated in the supragranular layers (L2/3) to pass the distance between the two recording electrodes.

For MUA detection, the wide-band signal was filtered (bandpass 300−3000 Hz) and negative events exceeding five standard deviations in amplitude were considered as action potentials. The spike frequency was analyzed prior to KCl application for 20 min (background MUA) and at the onset of the CSD wave (during 10 s before and 10 s after). To determine the time of recovery of neuronal activity after CSD, MUA was analyzed in L4 in the 10 min before, and 10 min after KCl application. MUA and LFP were detected and analyzed using MATLAB.

2.4. Behavioral tests

2.4.1. Von Frey test

Mechanical nociception was assessed using a series of calibrated Von Frey filaments with strength ranging from 0.008 to 0.6 g of target force, corresponding to 2.53–18.4 g/mm^2 pressure (Ugo Basile, Italy). Animals were placed individually in an acrylic cage with a mesh floor and allowed to acclimatize for 1 h until major grooming and exploration activities ceased. The “ascending stimulus” method was used to estimate the mechanical withdrawal threshold as previously described [20,33]. The von Frey filaments were applied at the whisker pad area in an ascending mode with an interval of 10 s between each filament. The first filament that evoked at least one response was assigned as the threshold.

2.4.2. Light/dark transition test

The light-dark box test was used to measure anxiety-like behavior [34]. The light–dark box consists of two equally-sized chambers - one illuminated (150 lx) and one darkened (1−2 lux) 40 × 20 × 40 cm/each connected with a passage way (7 × 7 cm) (Neurobotics, Russia) equipped with a video system Sony SSC-G118 (Japan). The rats were placed in the light compartment and allowed to explore the apparatus for 3 min. The following parameters were measured: latency to enter the dark chamber, the number of transitions between the light and dark chambers and time spent in the light chamber. After each trial the light-dark box was cleaned with 70 % ethanol and permitted to dry between tests.

2.4.3. Open field test

Locomotor behavior and anxiety were measured using Open field test [21]. This apparatus consists of a round arena 1 m in diameter with the floor divided into 19 parts and walls 0.4 m high (Open Science, Moscow, Russia) equipped with a video system Sony SSC-G118 (Japan). The central round area 20 cm in diameter was defined as a central zone and the other region was defined as the peripheral area. Each animal was placed in the middle of the open field for 10 min and the following parameters were evaluated: the first latency to exit the central zone, the number of line crossings (i.e., horizontal activity), rearing, defined as raising both forepaws above the floor while balancing on hind limbs and grooming episodes. Experiments and analysis of video images were done by different experimenters. After each trial the open field was cleaned with 70 % ethanol and permitted to dry between tests.

2.5. Statistical analysis

Electrophysiological and behavior data were analyzed using Origin Pro software (OriginLab Corp, Northampton, MA, USA). Statistical significance between groups was calculated using the Mann-Whitney test. Data are expressed as mean ± SEM. Differences were considered as statistically significant at $p < 0.05$; n indicates the number of animals.

3. Results

3.1. Electrophysiological recordings of CSD in control and hHCY groups

Topical application of KCl induced CSD across the cortical layers of somatosensory cortex (S1) recorded using a 16-site linear silicon probe (Fig. 1. C,D).

First, we compared the threshold for CSD induction in control versus hHCY rats by gradually elevating concentration of KCl. In control group, the threshold concentration of KCl to induce CSD was 100 mM (n = 4; Table 1). The animals with hHCY demonstrated higher susceptibility to CSD compared to the control group. In this case, the minimum KCl concentration required to induce CSD was 10–50 mM (n = 7; Table 1). On average, the KCl concentration inducing CSD in control was 300 ± 11 mM (n = 10) versus 60 ± 10 mM (n = 13, $p < 0.05$) in the hHCY group. Notably, CSD was detected in 46 % (10/24) of animals in control versus 57 % (13/23) of rats from the hHCY group.

Table 1
The threshold of KCl concentration for CSD induction in rats from the control and hHCY groups.

KCl concentration	Number of animals with CSD/all animals	Number of CSD (mean ± SEM)	Duration of CSDs occurrence (min) (mean ± SEM)
10 mM			
Control	0/10	0	
hHCY	1/13	1	
50 mM			
Control	0/10	0	
hHCY	6/13	1.1 ± 0.1	3.2 ± 1.0
100 mM			
Control	4/10	2.3 ± 0.4	8.4 ± 1.9
hHCY	13/13	2.6 ± 0.3	12.4 ± 1.6
200 mM			
Control	6/10	4.1 ± 0.6	14.3 ± 2.5
hHCY	13/13	3.7 ± 1.01	15.6 ± 4.0
300 mM			
Control	8/10	4.9 ± 0.9	14.2 ± 2.8
hHCY	12/13	3.6 ± 0.7	12.6 ± 3.0
600 mM			
Control	8/10	5.5 ± 1.2	15.3 ± 2.9
hHCY	13/13	6.3 ± 1.5	26.2 ± 6.2
1000 mM			
Control	8/10	7.7 ± 0.7	23.6 ± 4.5
hHCY	13/13	6.7 ± 1.7	20.4 ± 6.3

Next we characterized the vertical propagation of CSD within the cortical column. The earliest CSD onset was taken as T = 0 and the delays of CSD onsets from the earliest CSD onset were calculated for each recording channel of the probe (Fig. 1 E, F).

In control, the earliest CSD onset was in supragranular layers (L2/3, 9/10 rats) or in granular layer (L4, 1/10 rats) with an average depth of 350 ± 60 μm (n = 10). Likewise, in hHCY, the earliest CSD onset also mainly appeared in L2/3 (9/13 rats) and L4 (4/13 rats) but with an average depth of 480 ± 95 μm (n = 13, $p > 0.05$). Further, amplitude-time parameters were analyzed only in the CSD with earliest onset in the supragranular layers. On average the onsets of CSD within the cortical column were not significantly different in control and hHCY rats (Fig. 1 E, F).

CSD amplitudes in control increased from the supragranular to granular and infragranular layers reaching maximal values of ~30 mV (Fig. 2 A). In hHCY, CSD amplitudes in L4 were lower compared to control (Fig. 2 A).

The width (half-duration, $T_{1/2}$) of CSDs in the control group progressively shortened from the cortical surface to depth (Fig. 2 B). In contrast, in the hHCY group, a longer duration of CSD waves was observed in all cortical layers (Fig. 2 B). Thus, in supragranular layers the CSD duration was 28.3 ± 1.2 s in control (n = 9) versus 44.6 ± 1.2 s in the hHCY group (n = 9, $p < 0.05$). In granular layer the duration was 27.6 ± 1.0 s in control (n = 9) versus 37.8 ± 2.1 s in the hHCY group (n = 9; $p < 0.05$; Fig. 2 B).

Interestingly, the most striking difference between the control and hHCY groups was observed in the rise time and depolarization rate of CSD (Fig. 2 C,D). Thus, in control, the rise time of the first CSD was 4.4 ± 0.4 s in L2/3, 3.8 ± 0.2 s in L4, (n = 9) whereas in the hHCY group, the rise time of CSD was 8.4 ± 0.3 s in L2/3, 5.9 ± 0.3 s in L4 (n = 9, $p<0.05$) (Fig. 2 C). In addition, the depolarization rate of CSD in L2/3 and L4 in hHCY rats was lower compared to control (Fig. 2 D).

As an independent parameter of migraine-related cortical excitability, we measured the horizontal propagation of CSD generated in the supragranular layers using two recording electrodes (Fig. 3 A, inset). In control, the rate of CSD propagation was 3.7 ± 0.1 mm/min (n = 4) but

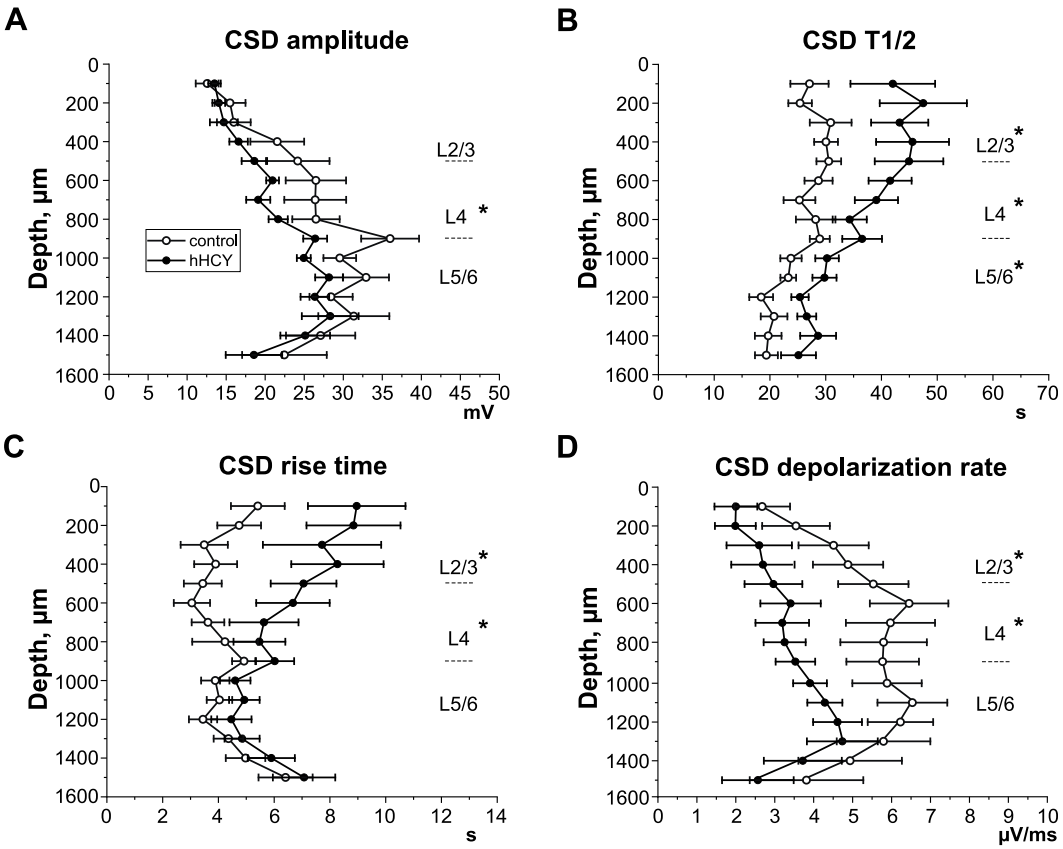

Fig. 2. Parameters of CSD at different cortical depths in rats from the control and hHCY groups. The average CSD amplitude (A), CSD half-duration (SD-$T_{1/2}$, B), rise time (C) and CSD depolarization rate (D) in different cortical layers in the control (white circles) and hHCY (black circles) groups. Data are expressed as mean ± SEM. *$p < 0$ 05 compared to the control group.

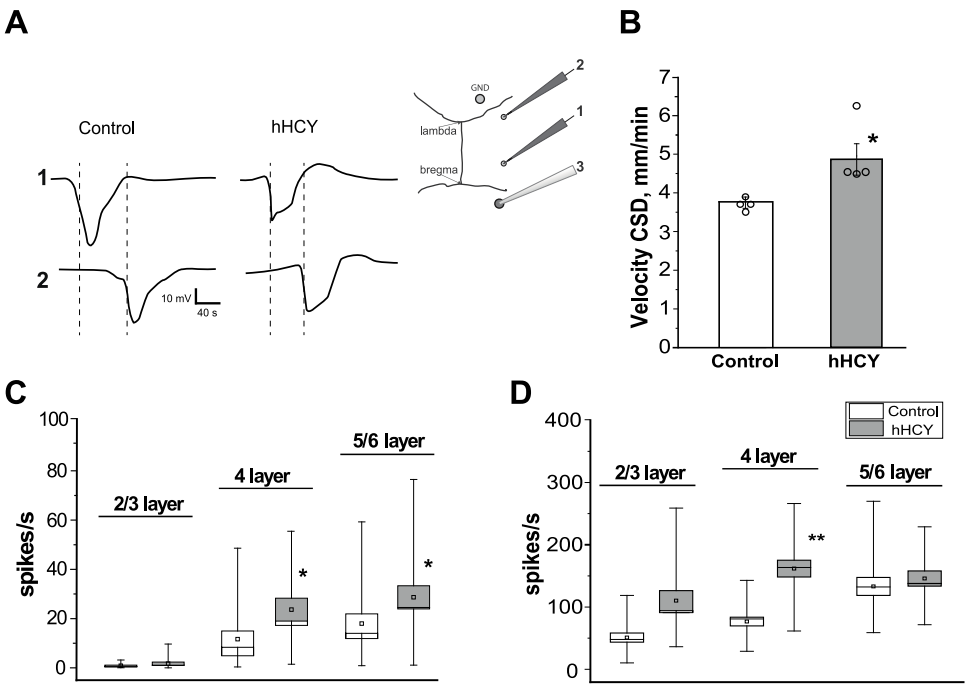

Fig. 3. CSD propagation and MUA frequency in different cortical layers in the control and hHCY groups. **A.** CSD, recorded in supragranular layers at two cortical points (1 and 2: 3.5 mm and 8 mm posterior and 4 mm lateral to bregma) in control and hHCY rats. KCl (0.3 M) (3) was applied in an additional hole in the frontal bone (5 mm anterior and 4 mm lateral to bregma). The ground electrode (GND) was placed in the visual cortex (experimental design is shown in the **inset**). The vertical dashed lines indicate the onset of CSD recorded by each electrode. The time necessary for CSD to propagate from the first to the second electrode was shorter in the hHCY group. **B.** Horizontal velocity of CSD in control and hHCY groups. Individual data points as well as mean ± SEM are shown for each experimental group. **C.** Background MUA frequency in cortical layers 2/3, 4 and 5/6 in control (white boxplot) and hHCY (grey boxplots) groups. Boxes indicate SEM, horizontal lines indicate median, the small square inside boxes indicate mean value, and whiskers indicate the 5-95 percentile of data. **D.** The increment of MUA frequency in cortical layers 2/3, 4 and 5/6 at the onset (during the 10 s before and 10 s after) of CSD compared to the background level.
*$p < 0\ 05$, ** $p < 0\ 01$ compared to the control group.

it was significantly higher in hHCY rats (4.9 ± 0.4 mm/min, n = 4; p < 0.05) (Fig.3 B).

As another independent index of neuronal excitability, we recorded the multi-unit activity (MUA) preceding CSD generation. MUA increased before CSD suggesting a growing excitability, but disappeared during depolarization, indicating a complete silence of electrical activity and then MUA slowly recovered in 5–10 min [35,36]. Analysis of MUA across the cortical layers before KCl application (background activity) and at the onset of CSD (10 s before and 10 s after) revealed neuronal hyperexcitability in rats with hHCY (Fig. 3 C, D). The background MUA in the granular and infragranular layers was significantly higher in the hHCY group. In L2/3 spike frequency was 0.8 ± 0.2 s^{-1} in control (n = 9) vs 1.6 ± 0.6 s^{-1} in the hHCY group (n = 9, p > 0.05); in L4 it was 11.7 ± 3.3 s^{-1} in control vs 22.7 ± 4.6 s^{-1} in hHCY group (p < 0.05); in L5/6 it was 17.4 ± 3.8 s^{-1} in control vs 32.2 ± 4.2 s^{-1} in the hHCY group (p < 0.05) (Fig. 3 C).

At the onset of CSD, MUA increased compared to the background values in all cortical layers (Fig. 3 D). However, in the hHCY group, the neuronal responses were higher compared to control, again, most visibly in L4 (Fig. 3 D). In L2/3 the increment of MUA was 47.4 ± 7.3 s^{-1} in the control group (n = 9) and 107.6 ± 16.5 s^{-1} in the hHCY group (n = 9, p > 0.05, Fig. 3 D). In L4 the increase MUA frequency in the hHCY group was significantly higher (182.3 ± 14.5 s^{-1}, p < 0.01) compared to control (84.1 ± 8.4 s^{-1}). In L5/6 the MUA frequency increased to the same extent in both groups (158.7 ± 20.5 s^{-1} in control and 171.6 ± 14.2 s^{-1} in the hHCY group (p > 0.05, Fig. 3D).

CSD wave generation induced a complete temporal loss of neuronal activity, recorded as absence of MUA, both in control and in hHCY rats. However, this functional spiking activity recovered in 5.9 ± 0.1 min in control (n = 9) versus a more slow recovery (7.5 ± 0.1 min) in the hHCY group (n = 9, p < 0.05).

Taken together, the electrophysiological recordings indicated significantly altered neuronal excitability and a predisposition to generation of the migraine-related phenomenon CSD in the cortex of rats with a sustained enhanced level of HCY.

3.2. Behavioral testing

3.2.1. Mechanical hypersensitivity

To evaluate the mechanical nociceptive threshold in rats with hHCY we examined head withdrawal in response to von Frey monofilaments applied to the whisker pad area. In the control group, the mechanical nociceptive threshold was 5.6 ± 0.4 g/mm^2 (n = 15), whereas in hHCY rats, the threshold was significantly lower (4.1 ± 0.3 g/mm^2, n = 15, p < 0.001; Fig. 4 A) indicating the development of mechanical hypersensitivity.

3.2.2. Light/dark transition test

The number of transitions between light and dark chambers was not different in both groups of animals (4.3 ± 1.1 in control vs 3.5 ± 1.1 8 in hHCY, p > 0.05, Fig. 4B). However, the first latency to enter the dark compartment was significantly lower in the hHCY group (33.3 ± 8.9 s, n = 15) than in the control group (83.8 ± 24.4 s, n = 15, p < 0.05) (Fig. 4 C). Similarly, the time spent in the light chamber during the observation period was higher in the control group (137.5 ± 10.4 s in control vs 106.1 ± 8.7 s in the hHCY group, n = 15; p < 0.05, Fig. 4 D). Taken together, these results indicated development of photophobia and anxiety.

3.2.3. Open field test

The locomotor activity of hHCY rats was measured as the number of crossed lines in the open field test. We found that this parameter was higher in rats from the hHCY group compared to the control group (42.6 ± 4.6 in control, n = 15 versus 61.3 ± 4.9 in hHCY, n = 15, p < 0.05) (Fig. 4 E). Rearing was not significantly different in the two experimental groups: 8.3 ± 1.2 in control versus 9.4 ± 1.4 events in hHCY group (p > 0.05, Fig. 4 F). The time spent in the central zone was longer in control (4.3 ± 0.4 s) compared to the hHCY group (2.6 ± 0.4 s, p < 0.05, Fig. 4 G). Likewise, the grooming behavior was increased in hHCY animals (2.6 ± 0.5 acts in control versus 4.3 ± 0.3 acts in hHCY, p < 0.05; Fig. 4 H).

In summary, the behavioral tests revealed that the typical features of migraine such as mechanical hyperalgesia and photophobia, as well as

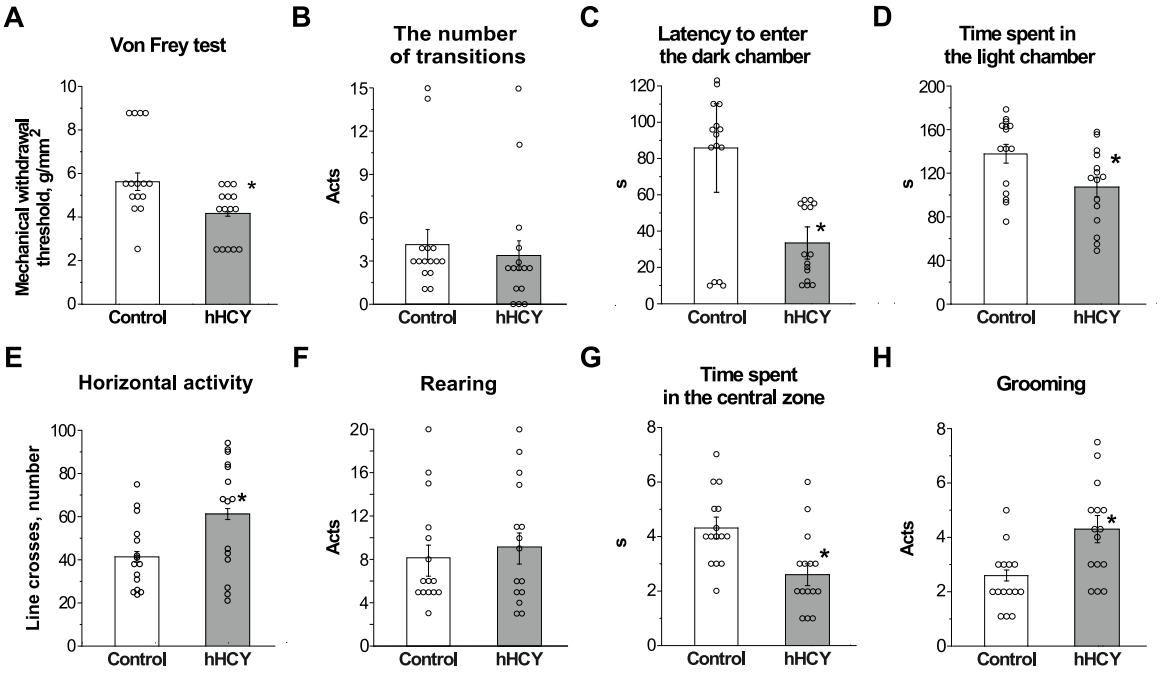

Fig. 4. Mechanical sensitivity, activity in the light/dark test and Open field test in rats from the control and hHCY groups Mechanical withdrawal threshold studied with von Frey filaments in the whisker pad of rats from the control and hHCY groups (A). Transitions between light and dark chambers (B), latency to enter the dark chamber (C) and time spent in the light chamber (D) of rats from the control and hHCY groups in Light/dark transition test. The number of line crosses (E), rearing (F), time spent in the central zone (G) and grooming acts (H) in the Open field test. Individual data points as well as mean ± SEM were shown for each experimental group. *$p < 0.05$ compared to the control group.

signs of anxiety, are associated with hHCY.

4. Discussion

In this study, for the first time, we provide a detailed analysis of electrical brain signaling in multiple layers of the cortex associated with migraine with aura in conditions of high level of the redox active amino acid HCY. These data are supported by the behavioral phenotype of animals with hHCY, which show mechanical allodynia, photophobia and anxiety, together a migraine related phenotype. In the somatosensory area of the brain of rats with prenatally acquired sustained hHCY, we found a reduced threshold for CSD induction and a higher velocity of horizontal CSD propagation. This fact suggests increased cortical excitability, which was further supported by a higher rate of background MUA and a larger increment of MUA preceding CSD. Moreover, in rats with hHCY, mechanical allodynia was observed in the facial area, indicating sensitization of the trigeminal nociceptive system known to be implicated in migraine pain. Finally, the open field and light/dark transition tests indicated development of photophobia and anxiety in animals with hHCY. The obtained data are consistent with view that hHCY is a risk factor for migraine with aura [4. 5, 11].

In our experiments, we used the rat model of prenatal hHCY, where a high HCY level was induced in dams by a methionine diet [24–26], which further induced low weight, persistent functional disabilities, and learning deficits in their offspring at the early and late stages of postnatal development [24–26,37]. Importantly, rats born from females with hHCY display an elevated HCY level throughout life even without additional methionine, probably due to an impaired methionine/HCY metabolic cycle in the perinatal period. This fact suggests the model we used is suitable for studying the association of elevated endogenous HCY with migraine symptoms.

As the underlying mechanism of migraine aura is believed to be CSD [13,14], we primarily focused on this phenomenon by employing a common model of CSD induced by KCl [38]. Male rats were used in our study due to dependence of CSD on the natural estrous cycle [39]. In particular, in mice the minimum potassium concentration required to evoke CSD in females was significantly lower in diestrus compared to proestrus, estrus, metestrus. At the same time threshold for CSD induction was similar in the other three phases and male animals [39]. We found that in rats from the hHCY group, the threshold KCl concentration for induction of CSD was about 5 times lower than in the control group, indicating a higher vulnerability of these animals to CSD. Moreover, horizontal CSD propagation was faster in animals with hHCY which indicates higher neuronal excitability [40]. Indeed, the background MUA and MUA burst preceding CSD was more prominent in the hHCY group which can be explained by changes in the intrinsic properties of neurons and glial cells and/or a disbalance of excitation and inhibition in the cortical circuits, facilitating CSD occurrence [41,42]. Similar changes in neuronal excitability were shown in the pyramidal neurons of hippocampal CA3 region in rats with prenatal hHCY [43]. HCY is known to be a potent excitatory neurotransmitter activating NMDA receptors [44,45], which play a key role in CSD initiation and propagation [46]. Upregulation of NMDA receptors or enhanced sensitivity to glutamate in hHCY conditions may explain the observed cortical changes [47].

The analysis of the vertical distribution of CSD demonstrated that the wave of depolarization propagated preferentially through the supragranular layers and then more slowly depolarized the granular and infragranular layers consistent with previous observations [29,48]. In rats from the hHCY group, the vertical propagation of CSD was similar to control, however a marked increase in rise time with a slower rate of depolarization was observed. In addition, CSD in hHCY displayed a lower amplitude and longer duration of CSD.

In healthy brain tissue, the propagation of CSD is accompanied by the cessation of spontaneous and evoked synaptic activity, which subsequently returns to normal. However, in pathological conditions such as head trauma, hypoxia/ischemia, and hypoglycemia, the recovery period is prolonged [49]. In our experiments, in the hHCY group, the MUA recovery period was significantly extended compared to the control group. This phenomenon is most likely explained by a delay in the re-establishment of ionic gradients and slower clearance of glutamate

due to the decreased activity of Na^+/K^+ ATPases observed in hHCY conditions [50].

Recent animal studies indicated possible relationships between behavior and susceptibility to CSD [21–23]. Such behavioral phenomena as mechanical allodynia and hyperalgesia frequently occur in the facial region in migraine patients and may extend to extracephalic regions [14,18,44]. Indeed, in our experiments, rats with prenatal hHCY demonstrated facial allodynia suggesting sensitization in the trigeminal nociceptive pathways [51,52]. The underlying mechanisms of peripheral sensitization in hHCY could be complex, including for instance, HCY-induced increased expression/activity of T-type Ca-channels [20] and/or activation of satellite glial cells [53].

Clinical studies have shown that depression and anxiety may increase the frequency of migraine attacks [15–17]. Depression and anxiety-like behaviors have been observed in rat chronic migraine models [23]. In our experiments, anxiety-like behavior was evaluated using the open-field and light/dark transition tests [54]. The open field test is a standard neophobic approach for detection of anxiety where rodents naturally tend to avoid the open space. In our study, animals with hHCY spent less time in the central zone of the open field, demonstrated higher horizontal activity, and more grooming events, they are thus considered to be more anxious compared to the control. Consistent with this, in the light/dark transition test hHCY rats avoided bright light suggesting photophobia and elevated anxiety [34]. The anxiety like behavior in rats with hHCY has previously been observed in our own, and other studies [26,55], and may be explained by imbalances in the levels of serotonin, dopamine, epinephrine and norepinephrine in the brain [55,56]. Thus, our data have shown that higher sensitivity to CSD is correlated with behavioral signs specific for chronic migraine model in rats with hHCY, specifically in males.

5. Conclusion

In conclusion, our electrophysiological data indicated that rats with an elevated plasma level of HCY have a higher susceptibility to the development of CSD which is considered a physiological correlate of aura in migraine. Animals with hHCY demonstrated a higher horizontal velocity of CSD, lower amplitude of CSD, and longer duration of CSD. With the behavioral tests, we revealed typical migraine related symptoms such as mechanical allodynia, photophobia and higher anxiety in rats with hHCY, suggesting the association of these symptoms with the higher risk of CSD. Taken together, our findings support a link between HCY and migraine with aura, this suggests that timely correction of the elevated HCY level in persons of the high risk group may be beneficial for treatment.

Funding

This work was supported by the Russian Science Foundation20-15-00100.

Author contributions

Elena Gerasimova: Conceptualization Investigation; Methodology, Formal analysis; Validation; Writing - original draft; Writing - review & editing; Gulshat Burkhanova, Kseniya Chernov, Nail Khaertdinov: Investigation; Andrey Zakharov: Formal analysis; Daniel Enikeev Investigation Visualization; Rashid Giniatullin: Conceptualization; Writing - original draft; Writing - review & editing; Guzel Sitdikova: Conceptualization, Funding acquisition, Project administration, Supervision, Writing - original draft; Writing - review & editing.

Declaration of Competing Interest

The authors declare no competing interests.

Acknowledgements

The authors would like to acknowledge Dr. Guzel Ziyatdinova for measurements of homocysteine concentration.

References

[1] R. Esse, M. Barroso, I.T. de Almeida, R. Castro, The contribution of homocysteine metabolism disruption to endothelial dysfunction: state-of-the-art, Int. J. Mol. Sci. 20 (4) (2019) 867, https://doi.org/10.3390/ijms20040867.
[2] R. Moretti, P. Caruso, The controversial role of homocysteine in neurology: from labs to clinical practice, Int. J. Mol. Sci. 20 (1) (2019) 231, https://doi.org/10.3390/ijms20010231.
[3] R. Ansari, A. Mahta, E. Mallack, L.J. Jun, Hyperhomocysteinemia and neurologic disorders: a review, J. Clin. Neurol. 10 (4) (2014) 281–288, https://doi.org/10.3988/jcn.2014.10.4.281.
[4] G. Lippi, C. Mattiuzzi, T. Meschi, G. Cervellin, L. Borghi, Homocysteine and migraine. A narrative review, Clin. Chim. Acta 433 (2014) 5–11, https://doi.org/10.1016/j.cca.2014.02.028.
[5] F. Cacciapuoti, Migraine homocysteine-related: old and new mechanisms, Neurology and Clinical Neurosci. 5 (2017) 137–140.
[6] L.M. Cupini, E. Stipa, Migraine aura status and hyperhomocysteinaemia, Cephalalgia 27 (7) (2007) 847–849, https://doi.org/10.1111/j.1468-2982.2007.01342.x.
[7] F. Moschiano, D. D'Amico, S. Usai, L. Grazzi, M. Di Stefano, E. Ciusani, et al., Homocysteine plasma levels in patients with migraine with aura, Neurol. Sci. 29 (2008) 173–175, https://doi.org/10.1007/s10072-008-0917-2.
[8] R. Hering-Hanit, N. Gadoth, A. Yavetz, S. Gavendo, B. Sela, Is blood homocysteine elevated in migraine? Headache 41 (8) (2001) 779–781, https://doi.org/10.1046/j.1526-4610.2001.01143.x.
[9] C. Isobe, Y. Terayama, A remarkable increase in total homocysteine concentrations in the CSF of migraine patients with aura, Headache 50 (2010) 1561–1569, https://doi.org/10.1111/j.1526-4610.2010.01713.x.
[10] S. Datta, S.K. Pal, H. Mazumdar, B. Bhandari, S. Bhattacherjee, S. Pandit, Homocysteine and cerebrovascular accidents, J. Indian Med. Assoc. 107 (2009) 345–346.
[11] I. Liampas, V. Siokas, A. Mentis, A. Aloizou, M. Dastamani, Z. Tsouris, et al., Serum homocysteine, pyridoxine, folate, and vitamin B12 levels in migraine: systematic review and meta-analysis, Headache (2020), https://doi.org/10.1111/head.13892.
[12] M. Lauritzen, J.P. Dreier, M. Fabricius, J.A. Hartings, R. Graf, A.J. Strong, Clinical relevance of cortical spreading depression in neurological disorders: migraine, malignant stroke, subarachnoid and intracranial hemorrhage, and traumatic brain injury, J. Cereb. Blood Flow Metab. 31 (2011) 17–35, https://doi.org/10.1038/jcbfm.2010.191.
[13] M.D. Ferrari, R.R. Klever, G.M. Terwindt, C. Ayata, A.M. van den Maagdenberg, Migraine pathophysiology: lessons from mouse models and human genetics, Lancet Neurol. 14 (1) (2015) 65–80, https://doi.org/10.1016/S1474-4422(14)70220-0.
[14] P.J. Goadsby, P.R. Holland, M. Martins-Oliveira, J. Hoffmann, S. Christoph, S. Akerman, Pathophysiology of migraine: a disorder of sensory processing, Physiol. Rev. 97 (2) (2017) 553–622, https://doi.org/10.1152/physrev.00034.2015.
[15] F. Baldacci, C. Lucchesi, M. Cafalli, M. Poletti, M. Ulivi, M. Vedovello, et al., Migraine features in migraineurs with and without anxiety–depression symptoms: a hospital-based study, Clin. Neurol. Neurosurg. 132 (2015) 74–78, https://doi.org/10.1016/j.clineuro.2015.02.017.
[16] M.F.P. Peres, J.P.P. Mercante, P.R. Tobo, H. Kamei, M.E. Bigal, Anxiety and depression symptoms and migraine: a symptom-based approach research, J. Headache Pain 18 (1) (2017) 37, https://doi.org/10.1186/s10194-017-0742-1.
[17] M. Nazeri, H.R. Ghahrechahi, A. Pourzare, F. Abareghi, S. Samiee-Rad, M. Shabani, et al., Role of anxiety and depression in association with migraine and myofascial pain temporomandibular disorder, Indian J. Dent. Res. 29 (5) (2018) 583–587, https://doi.org/10.4103/0970-9290.244932.
[18] G.E. Tietjen, J.L. Brandes, B.L. Peterlin, A. Eloff, R.M. Dafer, M.R. Stein, et al., Allodynia in migraine: association with comorbid pain conditions, Headache 49 (9) (2009) 1333–1344, https://doi.org/10.1111/j.1526-4610.2009.01521.x.
[19] R.B. Lipton, M.E. Bigal, S. Ashina, R. Burstein, S. Silberstein, M.L. Reed, et al., Cutaneous allodynia in the migraine population, Ann. Neurol. 63 (2) (2008) 148–158, https://doi.org/10.1002/ana.21211.
[20] A.S. Gaifullina, J. Lazniewska, E.V. Gerasimova, G.F. Burkhanova, Y. Rzhepetskyy, A. Tomin, et al., A potential role for T-type calcium channels in homocysteinemia-induced peripheral neuropathy, Pain. 160 (2019) 2798–2810, https://doi.org/10.1097/j.pain.0000000000001669.
[21] V.B. Bogdanov, O.V. Bogdanova, S.V. Koulchitskya, V. Chauvela, S. Multona, M. Y. Makarchuk, et al., Behaviour in the open field predicts the number of KCl-induced cortical spreading depressions in rats, Behav. Brain Res. 236 (1) (2013) 90–93, https://doi.org/10.1016/j.bbr.2012.08.004.
[22] Eda S. Francisco, R.C.A. Guedes, Neonatal taurine and alanine modulate anxiety-like behavior and decelerate cortical spreading depression in rats previously suckled under different litter sizes, Amino Acids 47 (11) (2015) 2437–2445, https://doi.org/10.1007/s00726-015-2036-8.
[23] M. Zhang, Y. Liu, M. Zhao, W. Tang, X. Wang, Z. Dong, et al., Depression and anxiety behaviour in a rat model of chronic migraine, J. Headache Pain 18 (1) (2017) 27, https://doi.org/10.1186/s10194-017-0736-z.

[24] E. Gerasimova, O. Yakovleva, G. Burkhanova, G. Ziyatdinova, N. Khaertdinov, G. Sitdikova, Effects of maternal hyperhomocysteinemia on the early physical development and neurobehavioral maturation of rat offspring, BioNanoScience. 7 (2017) 155–158, https://doi.org/10.1007/s12668-016-0326-6.
[25] O.V. Yakovleva, A.R. Ziganshina, S.A. Dmitrieva, A.N. Arslanova, A.V. Yakovlev, F. V. Minibayeva, et al., Hydrogen sulfide ameliorates developmental impairments of rat offspring with prenatal hyperhomocysteinemia, Oxid. Med. Cell. Longev. (2018), https://doi.org/10.1155/2018/2746873, 2746873.
[26] O. Yakovlev, A.K. Bogatova, R. Mukhtarova, A. Yakovlev, V. Shakhmatova, E. Gerasimova, et al., Hydrogen sulfide alleviates anxiety, motor, and cognitive dysfunctions in rats with maternal hyperhomocysteinemia via mitigation of oxidative stress, Biomolecules. 10 (7) (2020) 995, https://doi.org/10.3390/biom10070995.
[27] P.T. Lee, D. Lowinsohn, R.G. Compton, Simultaneous detection of homocysteine and cysteine in the presence of ascorbic acid and glutathione using a nanocarbon modified electrode, Electroanalysis. 26 (2014) 1488–1496, https://doi.org/10.1002/elan.201400091.
[28] G. Sitdikova, A. Zakharov, S. Janackova, E. Gerasimova, J. Lebedeva, A.R. Inacio, D. Zaynutdinova, M. Minlebaev, G.L. Holmes, R. Khazipov, Isoflurane suppresses early cortical activity, Ann. Clin. Transl. Neurol. 1 (1) (2014) 15–26, https://doi.org/10.1002/acn3.16. Epub 2013 Nov 20. PMID: 25356379; PMCID: PMC4207500.
[29] A. Nasretdinov, N. Lotfullina, D. Vinokurova, J. Lebedeva, G. Burkhanova, K. Chernova, et al., Direct current coupled recordings of cortical spreading depression using silicone probes, Front. Cell. Neurosci. 11 (2017) 408, https://doi.org/10.3389/fncel.2017.00408.
[30] J. Lebedeva, A. Zakharov, E. Ogievetsky, A. Minlebaeva, R. Kurbanov, E. Gerasimova, G. Sitdikova, R. Khazipov, Inhibition of Cortical Activity and Apoptosis Caused by Ethanol in Neonatal Rats In Vivo, Cereb. Cortex 27 (2) (2017) 1068–1082, https://doi.org/10.1093/cercor/bhv293. PMID: 26646511.
[31] H.S. Meyer, D. Schwarz, V.C. Wimmer, A.C. Schmitt, J.N. Kerr, B. Sakmann, M. Helmstaedter, Inhibitory interneurons in a cortical column form hot zones of inhibition in layers 2 and 5A, Proc. Natl. Acad. Sci. U. S. A. 108 (40) (2011) 16807–16812, https://doi.org/10.1073/pnas.1113648108. Epub 2011 Sep 26. PMID: 21949377; PMCID: PMC3189020.
[32] H. Toriumi, T. Shimizu, T. Ebine, T. Takizawa, Y. Kayama, A. Koh, et al., Repetitive trigeminal nociceptive stimulation in rats increases their susceptibility to cortical spreading depression, Neurosci. Res. 106 (2016) 74–78, https://doi.org/10.1016/j.neures.2015.12.0.
[33] J.R. Deuis, L.S. Dvorakova, I. Vetter, Methods used to evaluate pain behaviors in rodents, Front. Mol. Neurosci. 10 (2017) 284, https://doi.org/10.3389/fnmol.2017.00284.???.
[34] W. Toma, S.L. Kyte, D. Bagdas, Y. Alkhlaif, S.D. Alsharari, A.H. Lichtman, Z. J. Chen, E. Del Fabbro, J.W. Bigbee, D.A. Gewirtz, M.I. Damaj, Effects of paclitaxel on the development of neuropathy and affective behaviors in the mouse, Neuropharmacology 117 (2017) 305–315, https://doi.org/10.1016/j.neuropharm.2017.02.020. Epub 2017 Feb 22. PMID: 28237807; PMCID: PMC5489229.
[35] A. Leão, Spreading depression of activity in the cerebral cortex, J. Neurophysiol. 7 (6) (1944) 359–390, https://doi.org/10.1152/jn.1944.7.6.359.
[36] B. Larrosa, J. Pastor, L. López-Aguado, O. Herreras, A role for glutamate and glia in the fast network oscillations preceding spreading depression, Neuroscience 141 (2) (2006) 1057–1068, https://doi.org/10.1016/j.neuroscience.2006.04.005.
[37] S.A. Blaise, E. Nédélec, H. Schroeder, J.M. Alberto, C. Bossenmeyer-Pourié, J. L. Guéant, et al., Gestational vitamin B deficiency leads to homocysteine-associated brain apoptosis and alters neurobehavioral development in rats, Am. J. Pathol. 170 (2) (2007) 667–679, https://doi.org/10.2353/ajpath.2007.060339.
[38] A. Shatillo, K. Koroleva, R. Giniatullina, N. Naumenko, A.A. Slastnikova, R. R. Aliev, et al., Cortical spreading depression induces oxidative stress in the trigeminal nociceptive system, Neuroscience 253 (2013) 341–349, https://doi.org/10.1016/j.neuroscience.2013.09.002.
[39] T. Ebine, H. Toriumi, T. Shimizu, M. Unekawa, T. Takizawa, Y. Kayama, M. Shibata, N. Suzuki, Alterations in the threshold of the potassium concentration to evoke cortical spreading depression during the natural estrous cycle in mice, Neurosci. Res. 112 (2016) 57–62, https://doi.org/10.1016/j.neures.2016.06.001. Epub 2016 Jun 14. PMID: 27312532.
[40] D.S. de Lima, E.D. Francisco, C.B. Lima, R.C. Guedes, Neonatal L-glutamine modulates anxiety-like behavior, cortical spreading depression, and microglial immunoreactivity: analysis in developing rats suckled on normal size- and large size litters, Amino Acids 49 (2) (2017) 337–346, https://doi.org/10.1007/s00726-016-2365-2.
[41] K.M. Welch, Brain hyperexcitability: the basis for antiepileptic drugs in migraine prevention, Headache 45 (1) (2005) 25–32, https://doi.org/10.1111/j.1526-4610.2005.4501008.x.
[42] A. Tottene, R. Conti, A. Fabbro, D. Vecchia, M. Shapovalova, M. Santello, et al., Enhanced excitatory transmission at cortical synapses as the basis for facilitated spreading depression in Ca(v)2.1 knock in migraine mice, Neuron. 61 (2009) 762–773, https://doi.org/10.1016/j.neuron.2009.01.027.
[43] A.V. Yakovlev, E. Kurmashova, A. Zakharov, G.F. Sitdikova, Network-driven activity and neuronal excitability in hippocampus of neonatal rats with prenatal hyperhomocysteinemia, BioNanoScience. 8 (2018) 304–309, https://doi.org/10.1007/s12668-017-0450-y.
[44] S.A. Lipton, W.K. Kim, Y.B. Choi, S. Kumar, D.M. d'Emilia, P.V. Rayudu, et al., Neurotoxicity associated with dual actions of homocysteine at the N-methyl-D-aspartate receptor, Proc. Natl. Acad. Sci. U.S.A. 94 (1997) 5923–5928, https://doi.org/10.1073/pnas.94.11.5923.
[45] D.A. Sibarov, P.A. Abushik, R. Giniatullin, S.M. Antonov, GluN2A subunit containing NMDA receptors are the preferential neuronal targets of homocysteine, Front. Cell. Neurosci. 10 (2016) 246, https://doi.org/10.3389/fncel.2016.00246.
[46] A. Shatillo, R.A. Salo, R. Giniatullin, O.H. Gröhn, Involvement of NMDA receptor subtypes in cortical spreading depression in rats assessed by fMRI, Neuropharmacology. 93 (2015) 164–170, https://doi.org/10.1016/j.neuropharm.2015.01.028.
[47] P.K. Kamat, P. Kyles, A. Kalani, N. Tyagi, Hydrogen sulfide ameliorates homocysteine-induced Alzheimer's disease-like pathology, blood-brain barrier disruption, and synaptic disorder, Mol. Neurobiol. 53 (4) (2016) 2451–2467, https://doi.org/10.1007/s12035-015-9212-4.
[48] D. Kaufmann, J.J. Theriot, J. Zyuzin, C.A. Service, J.C. Chang, Y.T. Tang, et al., Heterogeneous incidence and propagation of spreading depolarizations, J. Cereb, Blood Flow Metab. 37 (5) (2017) 1748–1762, https://doi.org/10.1177/0271678X16659496.
[49] R.P. Kraig, C. Nicholson, Extracellular ionic variations during spreading depression, Neuroscience 3 (11) (1978) 1045–1059, https://doi.org/10.1016/0306-4522(78)90122-7.
[50] A. Rasić-Marković, O. Stanojlović, D. Hrncić, D. Krstić, M. Colović, V. Susić, T. Radosavljević, D. Djuric, The activity of erythrocyte and brain Na+/K+ and Mg2+-ATPases in rats subjected to acute homocysteine and homocysteine thiolactone administration, Mol. Cell. Biochem. 327 (1-2) (2009) 39–45, https://doi.org/10.1007/s11010-009-0040-6.
[51] M.L. Oshinsky, S. Gomonchareonsiri, Episodic dural stimulation in awake rats: a model for recurrent headache, Headache 47 (7) (2007) 1026–1036, https://doi.org/10.1111/j.1526-4610.2007.00871.x.
[52] M. Toyama, C. Kudo, C. Mukai, M. Inoue, A. Oyamaguchi, H. Hanamoto, et al., Trigeminal nervous system sensitization by infraorbital nerve injury enhances responses in a migraine model, Cephalalgia 37 (14) (2017) 1317–1328, https://doi.org/10.1177/0333102416678387.
[53] P.A. Abushik, M. Niittykoski, R. Giniatullina, A. Shakirzyanova, G. Bart, D. Fayuk, et al., The role of NMDA and mGluR5 receptors in calcium mobilization and neurotoxicity of homocysteine in trigeminal and cortical neurons and glial cells, J. Neurochem. 129 (2) (2014) 264–274, https://doi.org/10.1111/jnc.12615.
[54] D. Vuralli, A. Wattiez, F.R. Andrew, H. Bolay, Behavioral and cognitive animal models in headache research, J. Headache Pain 20 (1) (2019) 11, https://doi.org/10.1186/s10194-019-0963-6.
[55] M. Kumar, M. Modi, R. Sandhir, Hydrogen sulfide attenuates homocysteine-induced cognitive deficits and neurochemical alterations by improving endogenous hydrogen sulfide levels, BioFactors 43 (3) (2017) 434–450, https://doi.org/10.1002/biof.1354.
[56] L. Gao, X.N. Zeng, H.M. Guo, X.M. Wu, H.J. Chen, R.K. Di, et al., Cognitive and neurochemical alterations in hyperhomocysteinemic rat, Neurol. Sci. 33 (2012) 39–43, https://doi.org/10.1007/s10072-011-0645-x.